UNEXPECTED BEHAVIOUR OF FLAG AND S-CURVATURES ON THE INTERPOLATED POINCARÉ METRIC

SÁNDOR KAJÁNTÓ AND ALEXANDRU KRISTÁLY

Abstract. We endow the disc $D = \{(x_1, x_2) \in \mathbb{R}^2 : x_1^2 + x_2^2 < 4\}$ with a Poincaré-type Randers metric F_λ, $\lambda \in [0, 1]$, that 'linearly' interpolates between the usual Riemannian Poincaré disc model ($\lambda = 0$, having constant sectional curvature -1 and zero S-curvature) and the Finsler-Poincaré metric ($\lambda = 1$, having constant flag curvature $-1/4$ and constant S-curvature with isotropic factor $1/2$), respectively. Contrary to our intuition, we show that when $\lambda \nearrow 1$, both the flag and normalized S-curvatures of the metric F_λ *blow up* close to ∂D for some particular choices of the flagpoles.

1. Introduction

In Finsler geometry, both the *flag curvature* (replacing the sectional curvature from Riemannian geometry) and S*-curvature* (a typically Finslerian notion which gives the covariant derivative of the distortion along geodesics) play crucial roles in the study of various non-Riemannian phenomena. Unlike in Riemannian manifolds, Finsler manifolds with constant flag curvature and constant S-curvature (i.e., there exists an isotropic factor $c \in \mathbb{R}$ such that $S(x, y) = (n + 1)cF(x, y)$ for every $(x, y) \in TM$, where $n = \dim(M)$) are far to be fully classified. An important class of Finsler manifolds where these curvature notions can be efficiently analysed represents the *Randers metrics* that appear as solutions of the famous *Zermelo navigation problem*. Indeed, if (M, g) is a complete n-dimensional ($n \geq 2$) Riemannian manifold and W is a vector field on (M, g) describing the influence of the wind/current, the paths of optimal travel time appear as geodesics with respect to the metric defined by

$$F(x, y) = \sqrt{g_x(y, y)} + W_x(y), \qquad x \in M,\ y \in T_xM, \tag{1.1}$$

see Bao, Robles and Shen [2]. Metrics of the form (1.1) are called of Randers-type, which are typically Finsler metrics whenever $|W_x|_g = \sqrt{g^*_x(W_x, W_x)} < 1$ for every $x \in M$, where g^* stands for the co-metric of g. Although Randers metrics are well understood in a broad sense, see e.g. Cheng and Shen [3], surprising phenomena continuously appear as peculiar features of the non-Riemannian character of such structures, see e.g. Kristály and Rudas [5] and Shen [7, 8].

The present paper provides another surprising facts about the aforementioned curvatures of Randers spaces. For simplicity of presentation, we focus on a 2-dimensional case which is modelled on the disc

$$D = \{(x_1, x_2) \in \mathbb{R}^2 : x_1^2 + x_2^2 < 4\},$$

endowed with a special Randers metric

$$F_\lambda(x, y) = a(x)|y| + \lambda\langle\nabla b(x), y\rangle, \qquad x = (x_1, x_2) \in D,\ y = (y_1, y_2) \in T_xD = \mathbb{R}^2, \tag{1.2}$$

where $\lambda \in [0, 1]$ and $a, b \colon D \to [0, \infty)$ are the functions

$$a(x) = \frac{4}{4 - |x|^2} \quad \text{and} \quad b(x) = \ln\frac{4 + |x|^2}{4 - |x|^2}, \qquad x \in D. \tag{1.3}$$

Hereafter, $|\cdot|$ and $\langle\cdot, \cdot\rangle$ denote the usual norm and inner product in $\mathbb{R}^2$.

Date: 2020 December 22.
2000 *Mathematics Subject Classification.* Primary 53B40; Secondary 53C60.
Key words and phrases. Randers spaces; flag curvature; S-curvature; Finsler-Poincaré model.

We note that F_λ interpolates between two famous metrics. On one hand, for $\lambda = 0$ the metric in (1.2) reduces to the usual Riemannian Poincaré disc model having constant sectional curvature -1 and zero S-curvature. On the other hand, the metric (1.2) for $\lambda = 1$ turns out to be the Finsler-Poincaré metric of constant flag curvature $-1/4$ and constant S-curvature with isotropic factor $1/2$, investigated by Bao, Chern and Shen [1, §12.6]; we also note that in the 2-dimensional case, the flag curvature and Finslerian-Gaussian curvature coincide. Since the 1-form $W = \lambda \nabla b$ is closed for every $\lambda \in [0,1]$, it follows that the geodesics of F_λ are trajectory-wise the same as the geodesics of the underlying Riemannian metric $F_0(x,y) = a(x)|y|$, i.e., Euclidean circular arcs which meet the boundary ∂D at Euclidean right angles, and Euclidean straight rays that emanate from/toward the origin.

Having these particular features of the metric F_λ concerning the geodesics (for every $\lambda \in [0,1]$) and the curvatures (for $\lambda \in \{0,1\}$), the following natural question arises: are the flag and S-curvatures of F_λ constant for any $\lambda \in (0,1)$? After some computations we realized that the answers to these questions are negative.

Accordingly, – if we restrict our attention e.g. to the flag curvature, – we conjectured that there should be two bounded functions l_λ and u_λ serving as sharp upper and lower bounds of the flag curvature of F_λ for every $\lambda \in [0,1]$, with the ends $l_0 = u_0 = -1$ and $l_1 = u_1 = -1/4$. Surprisingly, it turns out that the lower bound l_λ is neither bounded nor continuous. More precisely, by using the notation $K_\lambda(x,y)$ for flag curvature with non-zero flagpole $y \in T_xD$ (noticing that the transverse edge is not relevant in the 2-dimensional case, see [1]) our first main result can be stated as follows:

Theorem 1.1. *Let $\lambda \in (0,1)$. Then*

$$l_\lambda = -\frac{1}{(1-\lambda)^2} < K_\lambda(x,y) < -\frac{1}{(1+\lambda)^2} = u_\lambda, \qquad \forall (x,y) \in TD \setminus \{0\}.$$

Furthermore, both inequalities are sharp; more precisely, for every $\alpha > 0$ one has

$$\lim_{|x| \nearrow 2} K_\lambda(x, -\alpha x) = l_\lambda \quad \textit{and} \quad \lim_{|x| \nearrow 2} K_\lambda(x, \alpha x) = u_\lambda.$$

Obviously, one has $\lim_{\lambda \searrow 0} K_\lambda(x,y) = -1$ for every $(x,y) \in TD \setminus \{0\}$. However, while the upper bound u_λ behaves as expected, the lower bound has an essential discontinuity at $\lambda = 1$, i.e.,

$$\lim_{\lambda \nearrow 1} \lim_{|x| \nearrow 2} K_\lambda(x, -\alpha x) = \lim_{\lambda \nearrow 1} l_\lambda = -\infty, \qquad \forall \alpha > 0. \tag{1.4}$$

Instead of S-curvature, we shall consider the *normalized S-curvature* $\overline{S}_\lambda = \frac{S_\lambda}{3F_\lambda}$ of the metric F_λ on $TD \setminus \{0\}$, $\lambda \in (0,1)$; in particular, whenever S_λ is isotropic (i.e. $S_\lambda(x,y) = 3c(x)F_\lambda(x,y)$), the isotropic factor $c(x)$ and $\overline{S}_\lambda$ coincide. Similarly to Theorem 1.1 we can state:

Theorem 1.2. *Let $\lambda \in (0,1)$. Then*

$$0 < \overline{S}_\lambda(x,y) < \frac{\lambda}{2(1-\lambda^2)} = w_\lambda, \qquad \forall (x,y) \in TD \setminus \{0\}.$$

Furthermore, both inequalities are sharp; more precisely, for every $\alpha > 0$ one has

$$\lim_{|x| \nearrow 2} \overline{S}_\lambda(x, \pm\alpha x) = 0 \quad \textit{and} \quad \lim_{|x| \nearrow 2} \overline{S}_\lambda\left(x, \alpha \mathcal{R}_\lambda^\pm(x)\right) = w_\lambda,$$

where $\mathcal{R}_\lambda^\pm \colon \mathbb{R}^2 \to \mathbb{R}^2$ stands for the rotation with angle $\pm \arccos(-\lambda)$ around the origin.

It is clear that $\lim_{\lambda \searrow 0} \overline{S}_\lambda(x,y) = 0$ for every $(x,y) \in TD \setminus \{0\}$, as expected. However,

$$\lim_{\lambda \nearrow 1} \lim_{|x| \nearrow 2} \overline{S}_\lambda\left(x, \alpha \mathcal{R}_\lambda^\pm(x)\right) = \lim_{\lambda \nearrow 1} w_\lambda = +\infty, \qquad \forall \alpha > 0, \tag{1.5}$$

thus for a specific setting the normalized S-curvature of F_λ blows up as well.

Relations (1.4) and (1.5) seem to be paradoxical with the behaviour of the usual Finsler-Poincaré metric F_1. However, these situations remind us to the density of the canonical measure of the interpolated metric F_λ, given by

$$\sigma_{F_\lambda}(x) = \frac{16}{(4-|x|^2)^2}\left(1-\frac{16\lambda^2|x|^2}{(4+|x|^2)^2}\right)^{\frac{3}{2}}, \qquad x \in D, \tag{1.6}$$

see Shen [6] and Farkas, Kristály and Varga [4]; indeed, while $\lim_{|x|\nearrow 2}\sigma_{F_1}(x) = 0$, it turns out that for every fixed $\lambda \in (0,1)$ the function σ_{F_λ} blows up close to the boundary ∂D (i.e., $|x| \nearrow 2$).

Usually, the explicit computation of the flag and S-curvatures is not an easy task, see e.g. Bao, Chern and Shen [1, §12.6]. However, another by-product of Theorems 1.1&1.2 is that we are able to develop an explicit computation for the curvatures of F_λ which could be instructive for further Randers metrics even in higher dimensions.

The paper is structured as follows. In Section 2 we provide a formula for the flag curvature of a 2-dimensional manifold endowed with a generic Randers metric given by (1.2). In Section 3 we turn our attention to the special case when $a, b\colon D \to (0,\infty)$ are defined by (1.3), establishing the precise dependence of the interpolated flag curvature K_λ by the parameter $\lambda \in [0,1]$. Finally, in Sections 3 and 4 we provide the proof of Theorems 1.1 and 1.2, i.e., we discuss the extrema of the flag curvature K_λ and normalized S-curvature $\overline{S}_\lambda$ with respect to the point $x \in D$, the direction of flagpole $y \in T_xD$ and parameter $\lambda \in [0,1]$.

2. Flag curvature formula for a class of special Randers spaces

In this section we deduce a general formula for the flag curvature of the 2-dimensional manifolds endowed with the (parameter-free) Randers metric

$$F(x,y) = a(x)|y| + \langle \nabla b(x), y\rangle, \qquad (x,y) \in TD, \tag{2.1}$$

where $a, b\colon D \to (0,\infty)$ are *arbitrarily* fixed smooth functions verifying the structural assumption $|\nabla b(x)| < a(x)$ for every $x \in D$; furthermore, when dealing with Theorems 1.1 and 1.2, we shall consider the parameter-depending case $b := \lambda b$ with $\lambda \in (0,1)$.

Throughout this section denote $L = \frac{F^2}{2}$. In case of a and b we use lower indexes to denote the partial derivatives with respect to the components of $x = (x_1, x_2) \in D$. In case of F we use lower indexes to denote the partial derivatives with respect to the components of $y = (y_1, y_2) \in \mathbb{R}^2$; for example, $a_1 = \frac{\partial a}{\partial x_1}$, $a_{12} = \frac{\partial^2 a}{\partial x_1 \partial x_2}$, $F_1 = \frac{\partial F}{\partial y_1}$, etc. Moreover, we use the usual summation convention $T_i y_i = T_1 y_1 + T_2 y_2$.

Our strategy is the following. In the first step we explicitly compute the metric tensor

$$g_{ij} = \frac{\partial^2 L}{\partial y_i \partial y_j}$$

and its inverse g^{ij}. In the next step we compute the geodesic spray coefficients

$$G^i = g^{ij}G_j, \quad \text{where} \quad G_j = \frac{\partial^2 L}{\partial x_k \partial y_j} y_k.$$

Finally we use the formula of the flag curvature from [1, relation (12.5.18)], given by

$$\begin{aligned} F^2K = {} & (\overline{G}^1_{x_1y_2} - \overline{G}^1_{x_2y_1})y_2 + (\overline{G}^2_{x_2y_1} - \overline{G}^2_{x_1y_2})y_1 \\ & + 2\left(\overline{G}^1\overline{G}^1_{y_1y_1} + \overline{G}^2\overline{G}^2_{y_2y_2} + \overline{G}^2\overline{G}^1_{y_1y_2} + \overline{G}^1\overline{G}^2_{y_2y_1}\right) \\ & - \left(\overline{G}^1_{y_1}\overline{G}^1_{y_1} + \overline{G}^2_{y_2}\overline{G}^2_{y_2} + 2\overline{G}^1_{y_2}\overline{G}^2_{y_1}\right), \end{aligned} \tag{2.2}$$

where $\overline{G}^i = \frac{G^i}{2}$, and the subscripts denote partial derivatives.

In our computations we frequently use the expressions of partial derivatives of F that we express below, i.e.,

$$\frac{\partial F}{\partial x_i} = a_i|y| + b_{si}y_s, \qquad \frac{\partial F}{\partial y_i} = a\frac{y_i}{|y|} + b_i$$

$$\frac{\partial^2 F}{\partial x_i \partial x_j} = a_{ij}|y| + b_{sij}y_s, \qquad \frac{\partial^2 F}{\partial x_i \partial y_j} = a_i\frac{y_j}{|y|} + b_{ji}, \qquad \frac{\partial^2 F}{\partial y_i \partial y_j} = a\frac{\delta_{ij}}{|y|} - a\frac{y_i y_j}{|y|^3}, \quad i,j \in \{1,2\}.$$

2.1. **Metric and co-metric.** The metric tensor can be written as

$$g_{ij} = \frac{\partial^2 L}{\partial y_i \partial y_j} = F_i F_j + F F_{ij} = \left(a\frac{y_i}{|y|} + b_i\right)\left(a\frac{y_j}{|y|} + b_j\right) + F \cdot \left(a\frac{\delta_{ij}}{|y|} - a\frac{y_i y_j}{|y|^3}\right);$$

in particular, one has

$$g_{11} = \left(a\frac{y_1}{|y|} + b_1\right)^2 + \frac{aFy_2^2}{|y|^3},$$

$$g_{22} = \left(a\frac{y_2}{|y|} + b_2\right)^2 + \frac{aFy_1^2}{|y|^3},$$

$$g_{12} = \left(a\frac{y_1}{|y|} + b_1\right)\left(a\frac{y_2}{|y|} + b_2\right) - \frac{aFy_1y_2}{|y|^3},$$

and

$$\det g = \frac{aF^3}{|y|^3}.$$

Its inverse g^{ij} has the components

$$g^{11} = \frac{|y|^3}{aF^3}\left(a\frac{y_2}{|y|} + b_2\right)^2 + \frac{y_1^2}{F^2},$$

$$g^{22} = \frac{|y|^3}{aF^3}\left(a\frac{y_1}{|y|} + b_1\right)^2 + \frac{y_2^2}{F^2},$$

$$g^{12} = -\frac{|y|^3}{aF^3}\left(a\frac{y_1}{|y|} + b_1\right)\left(a\frac{y_2}{|y|} + b_2\right) + \frac{y_1y_2}{F^2}.$$

2.2. **Geodesic spray coefficients.** Since

$$\frac{\partial L}{\partial x^k} = F\frac{\partial F}{\partial x^k} \quad \text{and} \quad \frac{\partial^2 L}{\partial x^k \partial y^s} = \frac{\partial F}{\partial x^k}\frac{\partial F}{\partial y^s} + F\frac{\partial^2 F}{\partial x^k \partial y^s},$$

we have

$$G_j = \frac{\partial^2 L}{\partial x_k \partial y_j}y_k - \frac{\partial L}{\partial x_j} = \frac{\partial F}{\partial y_j}\frac{\partial F}{\partial x_k}y_k + F\frac{\partial^2 F}{\partial x_k \partial y_j}y_k - F\frac{\partial F}{\partial x_j}$$

and

$$G^i = g^{ij}G_j = \frac{y_i}{F}\frac{\partial F}{\partial x_k}y_k + Fg^{ij}\left(\frac{\partial^2 F}{\partial x_k \partial y_j}y_k - \frac{\partial F}{\partial x_j}\right),$$

where we use relation $\frac{y_i}{F} = g^{ij}F_j$ that follows by Euler's theorem for homogeneous functions. We focus on the second term. Observe that

$$B_j = \frac{\partial^2 F}{\partial x_k \partial y_j}y_k - \frac{\partial F}{\partial x_j} = a_k\frac{y_j y_k}{|y|} + b_{jk}y_k - a_j|y| + b_{sj}y_s = a_k\frac{y_j y_k}{|y|} - a_j|y|;$$

in particular,

$$B_1 = \frac{y_2}{|y|}(a_2y_1 - a_1y_2) = \frac{y_2 D}{|y|} \qquad \text{and} \quad B_2 = \frac{y_1}{|y|}(a_1y_2 - a_2y_1) = -\frac{y_1 D}{|y|},$$

where $D = a_2y_1 - a_1y_2$. By using these expressions it yields that

$$F(g^{11}B_1 + g^{12}B_2) = \frac{D|y|^2F_2}{aF} \quad \text{and} \quad F(g^{21}B_1 + g^{22}B^2) = -\frac{D|y|^2F_1}{aF},$$

whence

$$G^1 = \frac{y_1}{F}\frac{\partial F}{\partial x_k}y_k + \frac{D|y|^2F_2}{aF},$$
$$G^2 = \frac{y_2}{F}\frac{\partial F}{\partial x_k}y_k - \frac{D|y|^2F_1}{aF}.$$

2.3. **Computation of flag curvature.** In the sequel we compute the flag curvature K by using formula (2.2) and certain computational/technical tricks. In our computations we use the following auxiliary notations:

$$u = \frac{1}{2}\frac{\partial F}{\partial x_k}y_k, \qquad v = \frac{D|y|^2}{2a}, \qquad p = y_1u + F_2v, \qquad q = y_2u - F_1v, \tag{2.3}$$

thus we have

$$\overline{G}^1 = \frac{p}{F} = \frac{y_1u + F_2v}{F} \quad \text{and} \quad \overline{G}^2 = \frac{q}{F} = \frac{y_2u - F_1v}{F}.$$

Since the first term of (2.2) involves derivatives with respect to $x = (x_1, x_2)$, while the latter two terms have only derivatives in $y = (y_1, y_2)$, we compute them in two separate steps. In the following computations, for p, q, u and v, we use lower indexes to denote partial derivatives with respect to y_i.

Step 1. We have

$$\overline{G}^1_{y_i} = \frac{p_iF - pF_i}{F^2} \quad \text{and} \quad \overline{G}^2_{y_i} = \frac{q_iF - qF_i}{F^2},$$

where

$$p_1 = u + y_1u_1 + F_{12}v + F_2v_1, \qquad q_1 = y_2u_1 - F_{11}v - F_1v_1,$$
$$p_2 = y_1u_2 + F_{22}v + F_2v_2, \qquad q_2 = u + y_2u_2 - F_{12}v - F_1v_2.$$

Accordingly, we have

$$\begin{aligned} e_1 &= (\overline{G}^1_{x_1y_2} - \overline{G}^1_{x_2y_1})y_2 + (\overline{G}^2_{x_2y_1} - \overline{G}^2_{x_1y_2})y_1 \\ &= \frac{\partial}{\partial x_1}\left(\overline{G}^1_{y_2}y_2 - \overline{G}^2_{y_2}y_1\right) + \frac{\partial}{\partial x_2}\left(\overline{G}^2_{y_1}y_1 - \overline{G}^1_{y_1}y_2\right) \\ &= \frac{\partial}{\partial x_1}\left(\frac{p_2y_2 - q_2y_1}{F} + \frac{F_2(qy_1 - py_2)}{F^2}\right) + \frac{\partial}{\partial x_2}\left(\frac{q_1y_1 - p_1y_2}{F} + \frac{F_1(py_2 - qy_1)}{F^2}\right) \end{aligned}$$

By Euler's theorem, it follows that

$$\begin{aligned} p_2y_2 - q_2y_1 &= (y_1u_2 + F_{22}v + F_2v_2)y_2 - (u + y_2u_2 - F_{12}v - F_1v_2)y_1 = Fv_2 - uy_1 \\ q_1y_1 - p_1y_2 &= (y_2u_1 - F_{11}v - F_1v_1)y_1 - (u + y_1u_1 + F_{12}v + F_2v_1)y_2 = -Fv_1 - uy_2 \\ qy_1 - py_2 &= (y_2u - F_1v)y_1 - (y_1u + F_2v)y_2 = -Fv, \end{aligned}$$

thus

$$\begin{aligned} e_1 &= \frac{\partial}{\partial x_1}\left(v_2 - \frac{uy_1}{F} - \frac{F_2v}{F}\right) + \frac{\partial}{\partial x_2}\left(-v_1 - \frac{uy_2}{F} + \frac{F_1v}{F}\right) \\ &= ((v_2)_{x_1} - (v_1)_{x_2}) - \frac{u_{x_1}y_1 + u_{x_2}y_2}{F} + \frac{u(y_1F_{x_1} + y_2F_{x_2})}{F^2} + \frac{v((F_1)_{x_2} - (F_2)_{x_1})}{F} \\ &\quad + \frac{F_1v_{x_2} - F_2v_{x_1}}{F} - \frac{v(F_1F_{x_2} - F_2F_{x_1})}{F^2}. \end{aligned} \tag{2.4}$$

Since $v=\frac{D|y|^2}{2a}$, where $D=a_2y_1-a_1y_2$, its partial derivatives can be expressed as

$$v_1=\frac{a_2(3y_1^2+y_2^2)-a_1(2y_1y_2)}{2a},\qquad v_2=\frac{a_2(2y_1y_2)-a_1(3y_2^2+y_1^2)}{2a},$$

$$v_{11}=\frac{3a_2y_1-a_1y_2}{a},\qquad v_{12}=\frac{a_2y_2-a_1y_1}{a},\qquad v_{22}=\frac{a_2y_1-3a_1y_2}{a}.$$

In the sequel we introduce the notations $D_b=b_2y_1-b_1y_2$, $w=a_{22}y_1^2+a_{11}y_2^2-a_{12}(2y_1y_2)$, and for any tensor T let $\widetilde{T}=\frac{\partial T}{\partial x_i}y_i$. Now let $\spadesuit_i$ be the i-th term in (2.4). We express each term separately, namely

$$\begin{aligned}
\spadesuit_1 &= (v_2)_{x_1}-(v_1)_{x_2}\\
&= \frac{(a_{12}(2y_1y_2)-a_{11}(3y_2^2+y_1^2))a-(a_2(2y_1y_2)-a_1(3y_2^2+y_1^2))a_1}{2a^2}\\
&\quad -\frac{(a_{22}(3y_1^2+y_2^2)-a_{12}(2y_1y_2))a-(a_2(3y_1^2+y_2^2)-a_1(2y_1y_2))a_2}{2a^2}\\
&= -\frac{\widetilde{\widetilde{a}}+3w}{2a}+\frac{\widetilde{a}^2+3D^2}{2a^2},\\
\spadesuit_2 &= -\frac{u_{x_1}y_1+u_{x_2}y_2}{F}=-\frac{F_{x_ix_j}y_iy_j}{2F}=-\frac{|y|\widetilde{\widetilde{a}}+\widetilde{\widetilde{\widetilde{b}}}}{2F},\\
\spadesuit_3 &= \frac{u(y_1F_{x_1}+y_2F_{x_2})}{F^2}=2\frac{u^2}{F^2}=\frac{(|y|\widetilde{a}+\widetilde{\widetilde{b}})^2}{2F^2},\\
\spadesuit_4 &= \frac{v((F_1)_{x_2}-(F_2)_{x_1})}{F}=\frac{v(a_2y_1+b_{12}|y|-a_1y_2-b_{12}|y|}{F|y|}=\frac{D^2|y|}{2aF},\\
\spadesuit_5 &= \frac{F_1v_{x_2}-F_2v_{x_1}}{F}=\frac{(ay_1+b_1|y|)}{|y|F}\frac{|y|^2((a_{22}y_1-a_{12}y_2)a-(a_2y_1-a_1y_2)a_2)}{2a^2}\\
&\quad -\frac{(ay_2+b_2|y|)}{|y|F}\frac{|y|^2((a_{12}y_1-a_{11}y_2)a-(a_2y_1-a_1y_2)a_1)}{2a^2}\\
&= \frac{a|y|w+b_1|y|^2(a_{22}y_1-a_{12}y_2)+b_2|y|^2(a_{11}y_2-a_{12}y_1)}{2aF}-\frac{a|y|D^2+D^2\widetilde{b}-DD_b\widetilde{a}}{2a^2F},\\
\spadesuit_6 &= -\frac{v(F_1F_{x_2}-F_2F_{x_1})}{F^2}=-\frac{v((ay_1+b_1|y|)(a_2|y|+\widetilde{b_2})-(ay_2+b_2|y|)(a_1|y|+\widetilde{b_1}))}{|y|F^2}\\
&= -\frac{D|y|(a|y|D+a(y_1\widetilde{b_2}-y_2\widetilde{b_1})+|y|^2(b_1a_2-b_2a_1)+|y|(b_1\widetilde{b_2}-b_2\widetilde{b_1}))}{2aF^2}.
\end{aligned}$$

Step 2. For further computations we need the following second order derivatives of G^i:

$$\begin{aligned}
\overline{G}^1_{y_1y_1} &= \frac{(p_{11}F-pF_{11})F-2(p_1F-pF_1)F_1}{F^3},\\
\overline{G}^1_{y_1y_2} &= \frac{(p_{12}F+p_1F_2-p_2F_1-pF_{12})F-2(p_1F-pF_1)F_2}{F^3},\\
\overline{G}^2_{y_2y_1} &= \frac{(q_{12}F+q_2F_1-q_1F_2-qF_{12})F-2(q_2F-qF_2)F_1}{F^3},\\
\overline{G}^2_{y_2y_2} &= \frac{(q_{22}F-qF_{22})F-2(q_2F-qF_2)F_2}{F^3},
\end{aligned}$$

where

$$
\begin{aligned}
p_{11} &= 2u_1 + y_1 u_{11} + F_{112} v + 2F_{12} v_1 + F_2 v_{11},\\
p_{12} &= u_2 + y_1 u_{12} + F_{122} v + F_{22} v_1 + F_{12} v_2 + F_2 v_{12},\\
q_{12} &= u_1 + y_2 u_{12} - F_{112} v - F_{11} v_2 - F_{12} v_1 - F_1 v_{12},\\
q_{22} &= 2u_2 + y_2 u_{22} - F_{122} v - 2F_{12} v_2 - F_1 v_{22}.
\end{aligned}
$$

Thus, one has

$$
\begin{aligned}
e_2 &= \overline{G}^1 \overline{G}^1_{y_1 y_1} + \overline{G}^2 \overline{G}^2_{y_2 y_2} + \overline{G}^2 \overline{G}^1_{y_1 y_2} + \overline{G}^1 \overline{G}^2_{y_2 y_1}\\
&= \frac{p}{F} \frac{(p_{11} F - p F_{11}) F - 2(p_1 F - p F_1) F_1}{F^3} + \frac{q}{F} \frac{(q_{22} F - q F_{22}) F - 2(q_2 F - q F_2) F_2}{F^3}\\
&\quad + \frac{q}{F} \frac{(p_{12} F + p_1 F_2 - p_2 F_1 - p F_{12}) F - 2(p_1 F - p F_1) F_2}{F^3}\\
&\quad + \frac{p}{F} \frac{(q_{12} F + q_2 F_1 - q_1 F_2 - q F_{12}) F - 2(q_2 F - q F_2) F_1}{F^3}\\
&= \frac{p p_{11} + q q_{22} + q p_{12} + p q_{12}}{F^2} - \frac{p^2 F_{11} + q^2 F_{22} + 2pq F_{12}}{F^3}\\
&\quad - \frac{2p p_1 F_1 + 2q q_2 F_2 + p q_1 F_2 + p q_2 F_1 + q p_1 F_2 + q p_2 F_1}{F^3} + 2\frac{(pF_1 + qF_2)^2}{F^4},\\
e_3 &= \overline{G}^1_{y_1} \overline{G}^1_{y_1} + \overline{G}^2_{y_2} \overline{G}^2_{y_2} + 2\overline{G}^1_{y_2} \overline{G}^2_{y_1}\\
&= \frac{p_1^2 + q_2^2 + 2p_2 q_1}{F^2} + \frac{(pF_1^2 + qF_2)^2}{F^4} - 2\frac{p p_1 F_1 + q q_2 F_2 + p q_1 F_2 + q p_2 F_1}{F^3}.
\end{aligned}
$$

We observe that

$$
\begin{aligned}
2e_2 - e_3 &= 2\frac{(p p_{11} + q q_{22} + q p_{12} + p q_{12})}{F^2} - \frac{p_1^2 + q_2^2 + 2p_2 q_1}{F^2} - 2\frac{p^2 F_{11} + q^2 F_{22} + 2pq F_{12}}{F^3}\\
&\quad - 2\frac{p p_1 F_1 + q q_2 F_2 + p q_2 F_1 + q p_1 F_2}{F^3} + 3\frac{(pF_1 + qF_2)^2}{F^4}.
\end{aligned} \tag{2.5}
$$

Now we may simplify $2e_2 - e_3$. Let $\clubsuit_i$ be the i-th term in (2.5). By using Euler's theorem for the 2-homogeneous function u and 3-homogeneous v in y, it turns out that

$$
\begin{aligned}
\clubsuit_1 &= 2\frac{p p_{11} + q q_{22} + q p_{12} + p q_{12}}{F^2} = \frac{1}{F^2}[16u^2 + 4u(F_2 v_1 - F_1 v_2)) + 8v(F_2 u_1 - F_1 u_2)\\
&\quad + 2v(F_{12} v_1 F_2 - F_{11} v_2 F_2 - F_{22} v_1 F_1 + F_{12} v_2 F_1) + 2v(v_{11} F_2^2 + v_{22} F_1^2 - 2v_{12} F_1 F_2)],\\
\clubsuit_2 &= -\frac{p_1^2 + q_2^2 + 2p_2 q_1}{F^2}\\
&= -\frac{1}{F^2}[10u^2 + 2u(F_2 v_1 - F_1 v_2) + 6v(u_1 F_2 - u_2 F_1) + 2v^2(F_{12}^2 - F_{11} F_{22})\\
&\quad + 2v(F_{12} F_2 v_1 + F_{12} F_1 v_2 - F_{22} F_1 v_1 - F_{11} F_2 v_2) + (F_2 v_1 - F_1 v_2)^2],\\
\clubsuit_3 &= -2\frac{p^2 F_{11} + q^2 F_{22} + 2pq F_{12}}{F^3} = -\frac{2v^2(F_2^2 F_{11} + F_1^2 F_{22} - 2F_1 F_2 F_{12})}{F^3},\\
\clubsuit_4 &= -2\frac{p p_1 F_1 + q q_2 F_2 + p q_2 F_1 + q p_1 F_2}{F^3} = -\frac{8u^2 + 2u(F_2 v_1 - F_1 v_2)}{F^2},\\
\clubsuit_5 &= 3\frac{(pF_1 + qF_2)^2}{F^4} = \frac{3u^2}{F^2}.
\end{aligned}
$$

In conclusion, it yields

$$
\begin{aligned}
2e_2 - e_3 = \frac{u^2}{F^2} - \frac{2v^2(F_2^2F_{11} + F_1^2F_{22} - 2F_1F_2F_{12})}{F^3} + \frac{2v(F_2u_1 - F_1u_2)}{F^2} \\
+ \frac{2v(v_{11}F_2^2 + v_{22}F_1^2 - 2v_{12}F_1F_2)}{F^2} - \frac{(F_2v_1 - F_1v_2)^2}{F^2}.
\end{aligned} \tag{2.6}
$$

Denoting the i-th term in (2.6) by $\diamondsuit_i$ we obtain

$$
\begin{aligned}
\diamondsuit_1 &= \frac{u^2}{F^2} = \frac{(\widetilde{a}|y| + \widetilde{\widetilde{b}})^2}{4F^2}, \\
\diamondsuit_2 &= -\frac{2v^2(F_2^2F_{11} + F_1^2F_{22} - 2F_1F_2F_{12})}{F^3} = -\frac{D^2|y|}{2aF}, \\
\diamondsuit_3 &= \frac{2v(F_2u_1 - F_1u_2)}{F^2} = \frac{D^2|y|}{2aF} + 2\spadesuit_6, \\
\diamondsuit_4 + \diamondsuit_5 &= \frac{2v(v_{11}F_2^2 + v_{22}F_1^2 - 2v_{12}F_1F_2)}{F^2} - \frac{(F_2v_1 - F_1v_2)^2}{F^2}, \\
&= \frac{D^2}{a^2} + \frac{3D^2D_b^2}{4a^2F^2} - \frac{\widetilde{a}^2}{4a^2} + \frac{\widetilde{a}DD_b}{2a^2F}.
\end{aligned}
$$

Summing up the spades and diamonds and performing some slight simplifications, it turns out that

$$
\begin{aligned}
F^2K = &-\frac{\widetilde{\widetilde{a}} + 3w}{2a} - \frac{|y|\widetilde{\widetilde{a}} + \widetilde{\widetilde{\widetilde{b}}}}{2F} + \frac{3(|y|\widetilde{a} + \widetilde{\widetilde{b}})^2}{4F^2} + \frac{a|y|w + b_1|y|^2(a_{22}y_1 - a_{12}y_2) + b_2|y|^2(a_{11}y_2 - a_{12}y_1)}{2aF} \\
&- \frac{3D|y|(a|y|D + a(y_1\widetilde{b_2} - y_2\widetilde{b_1}) + |y|^2(b_1a_2 - b_2a_1) + |y|(b_1\widetilde{b_2} - b_2\widetilde{b_1}))}{2aF^2} \\
&+ \frac{\widetilde{a}^2 + 10D^2}{4a^2} + \frac{DD_b\widetilde{a}}{a^2F} - \frac{D^2\widetilde{b}}{2a^2F} + \frac{3D^2D_b^2}{4a^2F^2}.
\end{aligned} \tag{2.7}
$$

One can see that the last formula contains w, D and variables with tilde. Our experience shows that performing those substitutions provide a formally more complicated formula. However, under some physically motivated, reasonable assumptions the above formula can be significantly simplified; we present this result in the next subsection.

2.4. **Effect of radial symmetry.** When the function $x \mapsto F(x,y)$ from (2.1) is radially symmetric for every $y \in \mathbb{R}^2$ (i.e., $a = a(|x|)$ and $b = b(|x|)$), we can assume without loss of generality that $x_2 = 0$, $y_1 = \cos t$, $y_2 = \sin t$. In that case we have $a_2 = a_{12} = b_2 = b_{12} = b_{112} = b_{222} = 0$. Under these assumptions (2.7) reduces to

$$
\begin{aligned}
F^2K = &-\frac{a_{11}(2a + b_1\cos t(1 + 2\sin^2 t)) + a_{22}(2a + 2b_1\cos t\cos^2 t)}{2aF} - \frac{b_{111}\cos^3 t + 3b_{122}\cos t\sin^2 t}{2F} \\
&+ \frac{4a^2a_1^2}{4a^2F^2} + \frac{2aa_1^2b_1\cos t(\cos^2 t + 11\sin^2 t)}{4a^2F^2} + \frac{a_1^2b_1^2\cos^2 t(\cos^2 t + 12\sin^2 t)}{4a^2F^2} + \frac{3a_1^2b_1^2\sin^4 t}{4a^2F^2} \\
&+ \frac{3(b_{11}\cos^2 t + b_{22}\sin^2 t)^2}{4F^2} + \frac{3a_1\cos t(b_{11}(\cos^2 t - \sin^2 t) + 2b_{22}\sin^2 t)}{2F^2} \\
&+ \frac{3a_1b_1b_{22}\sin^2 t}{2aF^2},
\end{aligned} \tag{2.8}
$$

where $x = (x_1, 0) \in D$ is the position and $y = (\cos t, \sin t)$ is the flagpole, with $t \in [0, 2\pi)$.

3. Behaviour of the flag curvature on the interpolated Poincaré metric

Let $\lambda \in [0,1]$. By using formula (2.8), we are going to express the flag curvature K_λ for the interpolating Poincaré metric (1.2) whenever the functions $a, b\colon D \to (0,\infty)$ are given by (1.3). For simplicity, let $\delta_- = \frac{1}{4-x_1^2}$, $\delta_+ = \frac{1}{4+x_1^2}$; thus $a = 4\delta_-$, $b_1 = 16x_1\delta_-\delta_+$ and the metric (1.2) reduces to

$$F_\lambda(x_1,t) = 4\delta_- + 16x_1\lambda\delta_-\delta_+\cos t, \qquad x_1 \in [0,2),\ t \in [0,2\pi).$$

Since the calculations are tedious, we only indicate the major steps and present the important intermediate results.

Step 1. We express the derivatives of a and b in terms of x_1, δ_+ and δ_-.

Step 2. Using these expressions (from Step 1) we substitute them into (2.8). After a suitable rearrangement of the terms, the resulting expression takes the form

$$K_\lambda = \frac{O_0 + O_1\lambda + O_2\lambda^2}{F_\lambda^4},$$

where

$$\begin{aligned}
O_0 &= -64\delta_-^3 - 64x_1^2\delta_-^4,\\
O_1 &= x_1\cos t\delta_-^2\delta_+\left(-448\delta_- + 192\delta_+\right) + x_1^3\cos t\delta_-^2\delta_+\left(-448\delta_-^2 - 192\delta_+^2\right)\\
&\quad + x_1^3\cos(3t)\delta_-^2\delta_+\left(-64\delta_-^2 - 128\delta_-\delta_+ - 64\delta_+^2\right),\\
O_2 &= x_1^4\cos(4t)\left(-32\delta_-^4\delta_+^2 - 64\delta_-^3\delta_+^3 - 32\delta_-^2\delta_+^4\right)\\
&\quad + x_1^2\cos(2t)\left(-768\delta_-^3\delta_+^2 - 896x_1^2\delta_-^4\delta_+^2 - 256x_1^2\delta_-^3\delta_+^3 - 128x_1^2\delta_-^2\delta_+^4\right)\\
&\quad + \left(192\delta_-^2\delta_+^2 - 96x_1^4\delta_-^4\delta_+^2 - 192x_1^4\delta_-^3\delta_+^3 - 96x_1^4\delta_-^2\delta_+^4\right).
\end{aligned}$$

Step 3. Using the expressions for δ_- and δ_+, it follows that

$$\begin{aligned}
K_\lambda(x_1,t) = &-\frac{4(4+x_1^2)^4}{4(4+x_1^2+4x_1\lambda\cos t)^4} - \frac{\lambda(16x_1\cos(t)(4+x_1^2)(16+20x_1^2+x_1^4) + 64x_1^3\cos(3t)(4+x_1^2))}{4(4+x_1^2+4x_1\lambda\cos t)^4}\\
&- \frac{\lambda^2(32x_1^4\cos(4t) + 16x_1^2(48+32x_1^2+3x_1^4)\cos(2t) - 3(256-64x_1^4+x_1^8))}{4(4+x_1^2+4x_1\lambda\cos t)^4}. \qquad (3.1)
\end{aligned}$$

We observe that for $\lambda \in \{0,1\}$, one has

$$K_0(x_1,t) = -1, \quad K_1(x_1,t) = -\frac{1}{4}, \qquad \forall x_1 \in [0,2),\ t \in [0,2\pi).$$

Hereafter, let $\lambda \in (0,1)$. We have

$$\begin{aligned}
\frac{\partial K_\lambda}{\partial x_1} = 0 &\iff \frac{(-16+x_1^4)\lambda(-1+\lambda^2)\cos t(16+x_1^4-8x_1^2\cos(2t))}{4+x_1^2+4x_1\lambda\cos t} = 0,\\
\frac{\partial K_\lambda}{\partial t} = 0 &\iff \frac{x_1(4+x_1^2)\lambda(-1+\lambda^2)(16+x_1^4-8x_1^2\cos(2t))\sin t}{4+x_1^2+4x_1\lambda\cos t} = 0.
\end{aligned}$$

The above equations show that the extremal values of K_λ occur when $t \in \{0,\pi/2,\pi,3\pi/2\}$ and either $x_1 = 0$, or $x_1 \nearrow 2$; on Figure 1 one can see both the special directions corresponding to these values and the evolution of $K_\lambda(x_1,t)$ by fixing different values of λ. We consider the following three cases:

Case 1: If the position $x = (x_1, 0)$ and the flagpole $y = (\cos t, \sin t)$ are orthogonal in the Euclidean sense, that is either $x_1 = 0$ or $t \in \{\pi/2, 3\pi/2\}$, then formula (3.1) reduces to

$$K_\lambda(0,\bar{t}) = K_\lambda(\bar{x}_1,\pi/2) = K_\lambda(\bar{x}_1,3\pi/2) = -1 + \frac{3\lambda^2}{4}, \qquad \forall \bar{x}_1 \in [0,2),\ \bar{t} \in [0,2\pi).$$

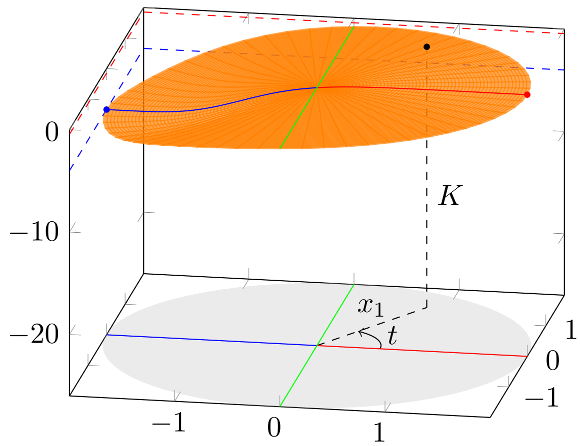

(A) $-4 < K_{1/2} < -4/9$; $K^T_{1/2} = -13/16$.

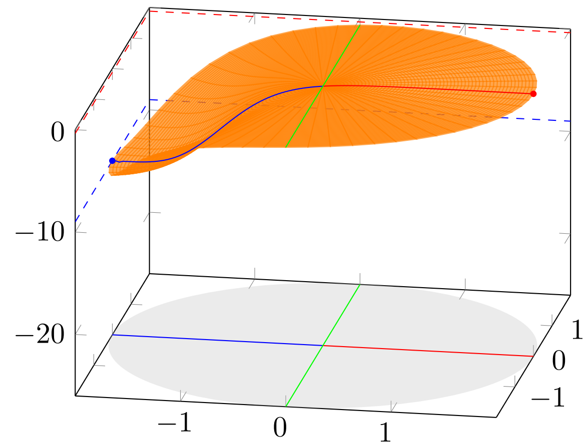

(B) $-9 < K_{2/3} < -9/25$; $K^T_{2/3} = -2/3$.

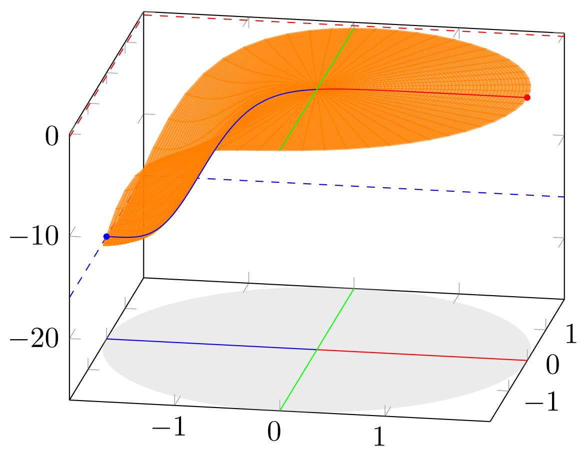

(C) $-16 < K_{3/4} < -16/49$; $K^T_{3/4} = -37/64$.

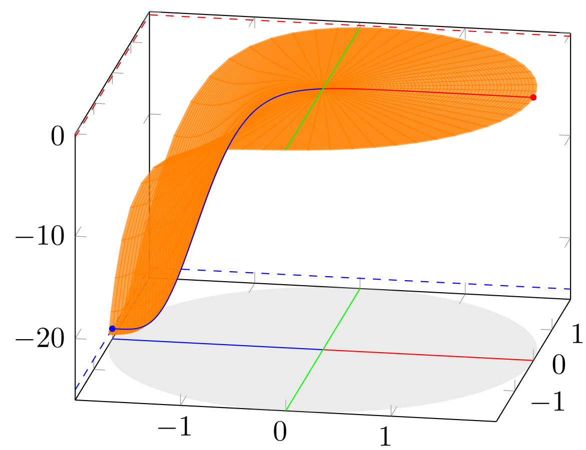

(D) $-25 < K_{4/5} < -25/81$; $K^T_{4/5} = -13/25$.

Figure 1. Representation of $K_\lambda(x_1, t)$ for the choices $\lambda \in \{1/2, 2/3, 3/4, 4/5\}$, where $t \in [0, 2\pi)$ and $x_1 \in [0, 2)$. The special directions $t \in \{\pi/2, 3\pi/2\}$ (green), $t = 0$ (red) and $t = \pi$ (blue) correspond to Cases 1-3, respectively. The sharp inequalities and the curvatures on transverse directions (K^T_λ) are presented as well. The 'valley' along the blue curve decreases to $-\infty$ whenever $\lambda \nearrow 1$, see also (1.4).

Case 2: If $x = (x_1, 0)$ approaches the rim of the disc and the flagpole points "outward", i.e., $x_1 \nearrow 2$ and $t = 0$, then

$$K_\lambda(2^-, 0) = -\frac{1}{(1+\lambda)^2}.$$

Case 3: If $x = (x_1, 0)$ approaches the rim of the disc and the flagpole points "inward", i.e., $x_1 \nearrow 2$ and $t = \pi$, then

$$\lim_{x_1 \nearrow 2} K_\lambda(x_1, \pi) = -\frac{1}{(1-\lambda)^2}.$$

Proof of Theorem 1.1. Cases 1-3 prove Theorem 1.1; indeed, since we provided sharp upper and lower bounds of K_λ, one has for every $\lambda \in (0, 1)$ that

$$-\frac{1}{(1-\lambda)^2} < K_\lambda(x_1, t) < -\frac{1}{(1+\lambda)^2}, \qquad \forall x_1 \in [0, 2),\ t \in [0, 2\pi).$$

We can also observe that when $\lambda \nearrow 1$ the lower bound tends to $-\infty$. □

4. Behaviour of the S-curvature on the interpolated Poincaré metric

According to Chern and Shen [9], the S-curvature of an n-dimensional Finsler manifold (M, F) can be calculated by

$$S = \frac{\partial \overline{G}^m}{\partial y_m} - y_m \frac{\partial}{\partial x_m} \ln \sigma_F,$$

where $\overline{G}^i = \frac{G^i}{2}$ are the geodesic spray coefficients and

$$\sigma_F(x) = \frac{\mathrm{Vol}(B^n(1))}{\mathrm{Vol}\{y \in T_xM : F(x,y) < 1\}}$$

is the density function of the natural measure ($B^n(1)$ denotes the Euclidean unit n-ball and Vol is the canonical Euclidean volume). In order to obtain an expression of degree zero, we normalize the S-curvature by considering $\frac{S}{(n+1)F}$ on $TM \setminus \{0\}$.

For the interpolated Poincaré metric (1.2) with functions $a, b : D \to \mathbb{R}$ from (1.3), the density function of the natural measure is

$$\sigma_{F_\lambda}(x) = a(x)^2 (1 - \lambda^2 |b|_a(x)^2)^{\frac{3}{2}},$$

where $a(x) = \frac{4}{4-|x|^2}$ and $|b|_a(x) = \frac{4|x|}{4+|x|^2}$, see (1.6).

Similarly to the previous sections without loss of generality we can assume that $x_2 = 0$, $y_1 = \cos t$, $y_2 = \sin t$, thus we get the following

$$\overline{S}_\lambda = \frac{S_\lambda}{3F_\lambda}(x,t) = \frac{\lambda(\overline{O}_0 + \overline{O}_1\lambda + \overline{O}_2\lambda^2)}{2((4+x_1^2)^2 - 16x_1^2\lambda^2)(4 + x_1^2 + 4x_1\lambda\cos t)^2},$$

where

$$\begin{aligned}
\overline{O}_0 &= (4+x_1^2)^2(16 + x_1^4 - 8x_1^2\cos(2t)) \\
\overline{O}_1 &= 8x_1(-4+x_1^2)^2(4+x_1^2)\cos t \\
\overline{O}_2 &= 16x_1^2(-8x_1^2 + (16+x_1^4)\cos(2t)).
\end{aligned}$$

We observe that if $\lambda = 0$ or $\lambda = 1$ then F_λ has constant S-curvature, since

$$\overline{S}_0(x_1,t) = 0, \quad \overline{S}_1(x_1,t) = \frac{1}{2}, \qquad \forall x_1 \in [0,2),\ t \in [0,2\pi).$$

Suppose that $\lambda \in (0,1)$. If extremal values of $\overline{S}_\lambda$ are attained then the following equations hold:

$$\begin{aligned}
\frac{\partial \overline{S}_\lambda}{\partial t} = 0 &\iff \frac{x_1(4+x_1^2)\lambda(-1+\lambda^2)(4x_1\lambda + (4+x_1^2)\cos t)\sin t}{((4+x_1^2)^2 - 16x_1^2\lambda^2)(4+x_1^2+4x_1\lambda\cos t)} = 0, \\
\frac{\partial \overline{S}_\lambda}{\partial x_1} = 0 &\iff \frac{x_1(x_1^4 - 16)\lambda(\lambda^2-1)\cos t \cdot T}{((4+x_1^2)^2 - 16x_1^2\lambda^2)(4+x_1^2+4x_1\lambda\cos t)} = 0,
\end{aligned}$$

where $T = (12x_1(4+x_1^2)^2\lambda + (4+x_1^2)((4+x_1^2)^2 + 48x_1^2\lambda^2)\cos t + 64x_1^3\lambda^3\cos(2t)) > 0$.

The second equation holds when $x_1 = 0$, $x_1 \nearrow 2$ or $\cos t = 0$, while the first equation holds when $x_1 = 0$, $\sin t = 0$, or both $x_1 \nearrow 2$ and $\cos t = -\lambda$; Figure 2 illustrates the special directions corresponding to these values and the evolution of $\overline{S}_\lambda(x_1,t)$ for various values of λ. The following three cases should be considered:

Case 1: If $x_1 = 0$, then

$$\overline{S}_\lambda(0,t) = \frac{\lambda}{2}, \qquad \forall t \in [0,2\pi).$$

We also observe that $\overline{S}_\lambda(x_1,\pi/2) = \overline{S}_\lambda(x_1,3\pi/2) = \frac{\lambda}{2}$, $\forall x_1 \in [0,2)$.

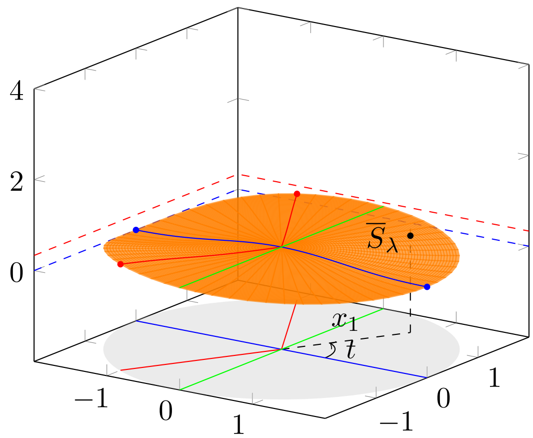

(A) $0 < \overline{S}_{1/2} < 1/3$; $\overline{S}^T_{1/2} = 1/4$; $t_{\max} \approx 2.09$.

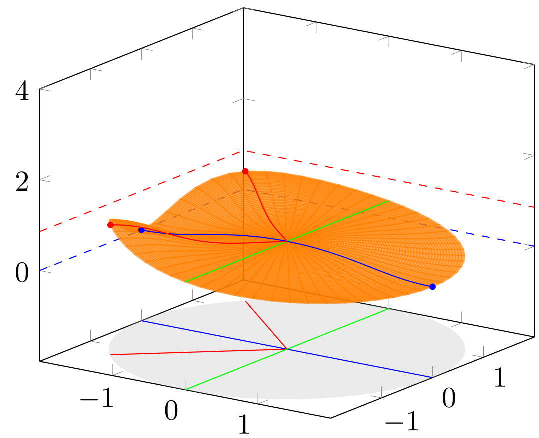

(B) $0 < \overline{S}_{3/4} < \frac{6}{7}$; $\overline{S}^T_{3/4} = 3/8$; $t_{\max} \approx 2.42$.

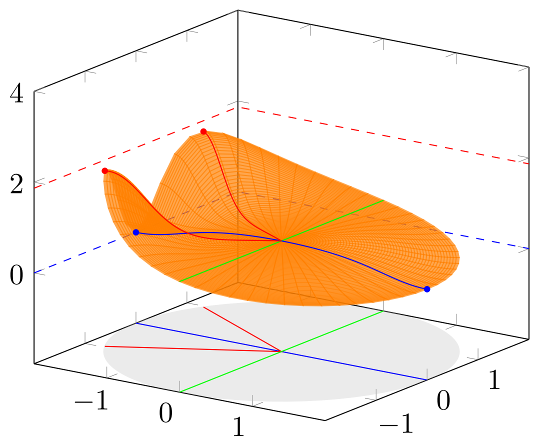

(C) $0 < \overline{S}_{7/8} < \frac{28}{15}$; $\overline{S}^T_{7/8} = 7/16$; $t_{\max} \approx 2.64$.

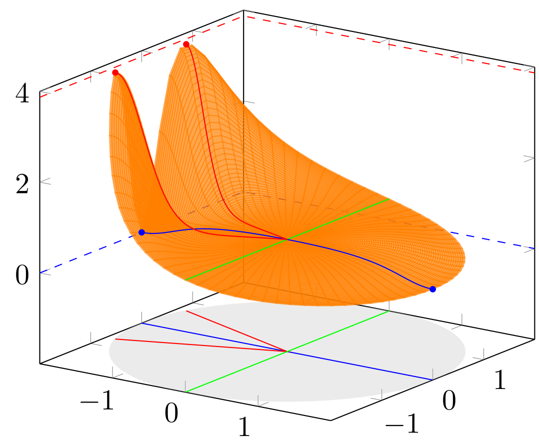

(D) $0 < \overline{S}_{15/16} < \frac{120}{31}$; $\overline{S}^T_{15/16} = 45/32$; $t_{\max} \approx 2.79$.

FIGURE 2. Representation of $\overline{S}_\lambda(x_1,t)$ for the choices $\lambda \in \{1/2, 3/4, 7/8, 15/16\}$, where $t \in [0, 2\pi)$ and $x_1 \in [0, 2)$. The special directions $t \in \{\pi/2, 3\pi/2\}$ (green), $t \in \{\arccos(-\lambda), 2\pi - \arccos(-\lambda)\}$ (red) and $t \in \{0, \pi\}$ (blue) correspond to Cases 1-3, respectively. The sharp inequalities, the curvatures on transverse directions ($\overline{S}^T_\lambda$) and the values $t_{\max} = \arccos(-\lambda)$ (in radian) are presented as well. The 'peaks' along the red curves increase to $+\infty$ whenever $\lambda \nearrow 1$, see also (1.5).

Case 2: If $x_1 \nearrow 2$ and $\cos t = -\lambda$, then

$$\lim_{x_1 \nearrow 2} \overline{S}_\lambda(x_1,t) = \frac{\lambda}{2(1-\lambda^2)}.$$

Case 3: If $x_1 \nearrow 2$ and $\sin t = 0$, then

$$\lim_{x_1 \nearrow 2} \overline{S}_\lambda(x_1,t) = 0.$$

Proof of Theorem 1.2. The above Cases 1-3 prove Theorem 1.2. Since we provided sharp upper and lower bounds of $\overline{S}_\lambda$, one has for every $\lambda \in (0,1)$ that

$$0 < \overline{S}_\lambda(x_1,t) < \frac{\lambda}{2(1-\lambda^2)}, \qquad \forall x_1 \in [0,2),\ t \in [0,2\pi).$$

We can also observe that when $\lambda \nearrow 1$ the upper bound tends to $+\infty$. $\square$

Acknowledgement. Research of A. Kristály is supported by the National Research, Development and Innovation Fund of Hungary, financed under the K_18 funding scheme, Project No. 127926.

References

[1] D. Bao, S.-S. Chern, Z. Shen, An introduction to Riemann-Finsler geometry. Graduate Texts in Mathematics, 200. Springer-Verlag, New York, 2000.
[2] D. Bao, C. Robles, Z. Shen, Zermelo navigation on Riemannian manifolds. *J. Differential Geom.* 66 (2004), no. 3, 377–435.
[3] X. Cheng, Z. Shen, Finsler geometry. An approach via Randers spaces. Science Press Beijing, Beijing; Springer, Heidelberg, 2012.
[4] C. Farkas, A. Kristály, C. Varga, Singular Poisson equations on Finsler-Hadamard manifolds. *Calc. Var. Partial Differential Equations* 54 (2015), no. 2, 1219–1241.
[5] A. Kristály, I.J. Rudas, Elliptic problems on the ball endowed with Funk-type metrics. *Nonlinear Anal.* 119 (2015), 199–208.
[6] Z. Shen, Lectures on Finsler Geometry, World Scientific Publishing Co., Singapore, 2001.
[7] Z. Shen, Projectively flat Finsler metrics of constant flag curvature. Trans. Amer. Math. Soc. 355 (4)(2003), 1713–1728.
[8] Z. Shen, Finsler metrics with $K = 0$ and $S = 0$. Canad. J. Math.55(2003), no.1, 112–132.
[9] S.-S. Chern, Z. Shen, Riemann-Finsler Geometry, World Scientific, Singapore, 2005.

Department of Mathematics, Babeş-Bolyai University, Cluj-Napoca, Romania
E-mail address: kajanto.sandor@math.ubbcluj.ro

Department of Economics, Babeş-Bolyai University, Cluj-Napoca, Romania & Institute of Applied Mathematics, Óbuda University, Budapest, Hungary
E-mail address: alexandru.kristaly@ubbcluj.ro; kristaly.alexandru@nik.uni-obuda.hu